

Parameter Inference in the Pulmonary Circulation of Mice

L. Mihaela Paun¹, M. Umar Qureshi², Mitchel Colebank²,
Mansoor A. Haider², Mette S. Olufsen², Nicholas A. Hill¹, Dirk
Husmeier¹

¹ School of Mathematics and Statistics, University of Glasgow, Glasgow G12
8SQ, UK

² Department of Mathematics, NC State University, Raleigh, NC 27695, USA

E-mail for correspondence: 1.paun.1@research.gla.ac.uk

Abstract: This study focuses on parameter inference in a pulmonary blood circulation model for mice. It utilises a fluid dynamics network model that takes selected parameter values and aims to mimic features of the pulmonary haemodynamics under normal physiological and pathological conditions. This is of medical relevance as it allows monitoring of the progression of pulmonary hypertension. Constraint nonlinear optimization is successfully used to learn the parameter values.

Keywords: Pulmonary hypertension; Parameter Inference; Constraint Nonlinear Optimization; Partial Differential Equations; Windkessel model.

1 Introduction

Pulmonary hypertension (PH) is a leading cause of right heart failure. It involves vascular remodelling including stiffening of the large and small arteries. Clinically, PH is diagnosed by analysing blood pressure (BP) measured invasively in the large pulmonary arteries. However, key parameters, including arterial stiffness, cannot be measured *in vivo*. This creates the need for methods to estimate parameters indirectly from the measured haemodynamic blood flow and pressure data. This study uses a 1D fluid dynamical network model that predicts blood flow and pressure in the large pulmonary arteries (for details see Qureshi et al., 2017). The model is used to predict blood flow and pressure in healthy and hypoxic mice, for which

This paper was published as a part of the proceedings of the 32nd International Workshop on Statistical Modelling (IWSM), Johann Bernoulli Institute, Rijksuniversiteit Groningen, Netherlands, 3–7 July 2017. The copyright remains with the author(s). Permission to reproduce or extract any parts of this abstract should be requested from the author(s).

data were acquired invasively (Tabima et al., 2012). The method discussed here is not specific to mice, but can easily be extended to analysis of similar data from humans for whom repeated invasive procedures are required for diagnosis and treatment. The ultimate goal, and hence the motivation behind inferring the parameters, is to minimise the number of invasive procedures for PH patients, as well as to assist clinicians in devising better treatment strategies. Thus, this study focuses on inference of key parameters pertinent to disease detection and treatment. We show that using this statistical method, BP prediction is improved in healthy and hypoxic mice compared to the reference prediction obtained by using the best parameter guesses in Qureshi et al. (2017). This leads to enhanced reliability of key parameter estimates obtained using the model.

2 Mathematical Model

The 1D fluid-structure model is derived from the incompressible axisymmetric Navier–Stokes equations for a Newtonian fluid, coupled with a constitutive wall model predicting stiffness of the blood vessels. In addition, assuming that the vessels are cylindrical and the wavelength is significantly longer than their radii, conservation of mass and momentum give

$$\frac{\partial A}{\partial t} + \frac{\partial q}{\partial x} = 0, \quad \frac{\partial q}{\partial t} + \frac{\partial}{\partial x} \frac{q^2}{A} + \frac{A}{\rho} \frac{\partial p}{\partial x} = -\frac{2\pi\mu r}{\delta} \frac{q}{A}, \quad (1)$$

where x (cm) and t (s) are the axial and temporal coordinates, p (mmHg) is blood pressure, q (ml/s) is blood flow rate, A (cm²) is the cross-sectional area, $\delta = 40 \mu\text{m}$ is the thickness of Stokes-layer in velocity profile, $\rho = 1.055 \text{ g/ml}$ is the blood density and $\mu = 0.0528 \text{ cm}^2/\text{s}$ is the viscosity. Assuming the arterial walls are homogeneous, isotropic and thin, the pressure-area relation is given by

$$p - p_0 = \frac{4}{3} \frac{Eh}{r_0} \left(1 - \sqrt{\frac{A_0}{A}} \right) \implies c^2(p) = \frac{A}{\rho} \frac{\partial p}{\partial A} = \frac{2}{3\rho} \frac{Eh}{r_0} \sqrt{\frac{A_0}{A}}, \quad (2)$$

where c (cm/s) is the wave speed, A_0 is the vessel cross-sectional area and r_0 (cm) the vessel radius at the pressure p_0 .

The arterial network geometry, including length and radii for the 13 largest vessels in the pulmonary vasculature is obtained from a micro CT image of a healthy mouse lung (see Figure 1(a)). To solve the equations, boundary conditions are specified at the inlet and outlet vessels in the network. The system is driven by imposing an invasively measured flow profile at the inlet of the main pulmonary artery (MPA), while conservation of blood flow and continuity of pressure are enforced across the bifurcations. For the outflow boundary conditions, 3-element Windkessel models (two resistors R_1, R_2 and a capacitor C) are attached to the outlet of each of the seven

terminal arteries in the network. The outflow boundary conditions account for the lumped effects of pulmonary haemodynamics beyond the truncated network of large arteries. The Windkessel model relates flow and pressure in the time domain over a cardiac cycle of length T via the input impedance $Z(\omega)$ by:

$$Z(\omega) = R_1 + \frac{R_2}{1 + i\omega CR_2} \implies q(L, t) = \frac{1}{T} \int_0^T p(L, t - \tau) Z(\tau) d\tau, \quad (3)$$

where R_1 and R_2 are the proximal and distal vascular resistances beyond each truncated artery, $R_1 + R_2$ is the total resistance and C is the total compliance of the vascular bed. The model takes a number of parameters as input and predicts the flow and pressure at different locations along the large pulmonary arteries. One of these parameters is the arterial stiffness, which significantly increases during the PH and which can be expressed as follows: $\frac{Eh}{r_0} = f_1 \exp(f_2 r_0) + f_3$, where E and h are the Young's modulus and thickness of the arterial wall, and f_1 (g cm/s^2), f_2 (cm^{-1}), f_3 (g cm/s^2) are the material parameters.

3 Methodology

Let the statistical model be defined by $y_i = f(x_i; \boldsymbol{\theta}) + \epsilon_i$, where $y_i \in \mathbf{y}$ are the noisy measured flow and pressure, $f(\cdot)$ describes the system behaviour that comes from numerically solving the fluids model, $\boldsymbol{\theta}$ are the parameters that we wish to infer from the observed flow and pressure and they are bounded, $x_i \in \mathbf{x}$ denote other input variables and ϵ are the errors, which we assume are i.i.d and follow a Gaussian distribution. The objective function to be minimised using Constraint Nonlinear Optimization is the Residual Sum of Squares,

$$RSS = \sum_i (y_i - f(x_i; \boldsymbol{\theta}))^2. \quad (4)$$

Under the assumption of i.i.d. Gaussian errors, the log likelihood of the data takes the form

$$\log(L) = -n \log \sqrt{2\pi\sigma^2} - \frac{RSS}{2\sigma^2}. \quad (5)$$

A Sequential Quadratic Programming (SQP) gradient-based method is used to minimise the RSS (Boggs et al., 2000).

4 Simulations

Simulations are set up to mimic experimental waveforms, which are recorded in the MPA in healthy and hypoxic mice (Tabima et al., 2012). The parameter set to be inferred initially includes $\boldsymbol{\theta} = (\frac{Eh}{r_0}, r_1, r_2, c_1)$, where r_1, r_2

are resistances ($r_1 = (1 - 0.5r_1)R_{01}$, $r_2 = (1 - 0.5r_2)R_{02}$, R_{01} and R_{02} are nominal resistances) and c_1 capacitance ($C = (1 - 0.5c_1)C_0$, C_0 is nominal capacitance) used to predict parameters assigned at the outlet and $\frac{Eh}{r_0}$ is the elastance used to predict stiffness in all vessels. The parameter set is subsequently extended to include a tapering factor, ζ , for the large vessels in the network, as there was evidence of vessel radii decreasing along their length, but this was not quantified during the segmentation process. Since the parameters are on different scales ($\frac{Eh}{r_0} \in [2.424 \times 10^5, 6.85 \times 10^6]$, $r_1, r_2, c_1 \in [-2, 2]$, and $\zeta \in [0, 1.2]$), to avoid having an ill-conditioned problem induced by a high condition number in the Hessian matrix, we rescale the parameters to have the same order of magnitude (Yang et al., 2010). Certain parameter configurations violate the model assumptions; these are marked by setting RSS to a high value (10^{10}). The RSS is calculated for pressure and we aim to find the set of parameters that minimise the RSS. The initial parameter values are uniformly drawn from a Sobol sequence to ensure a good coverage of the multidimensional parameter space (Bratley et al., 1988). The algorithm is iterated until it satisfies the convergence criterion, i.e. $|\theta_i - \theta_{i+1}| < 10^{-11}$. One forward simulation of the mathematical model takes 13 seconds to complete. The optimization problem required 3 hours on average to reach convergence of parameter estimates.

5 Results and Discussion

Regardless of the initial value, the algorithm converged for both the healthy and the hypoxic mouse studied. Figure 1 shows our optimised pressure waveform, plotted alongside the measured and the reference pressure for the 4D optimization problem. Panel (d) shows the pressure fit for the hypoxic mouse. The optimized fit predicts data better than nominal parameter values, supported by a significantly smaller RSS than the one between the reference and the measured pressure (panel (b)). For the healthy mouse (panel (c)), the simulated pressure closely follows the measured pressure except near the peak, where an offset is registered. Nevertheless, in this case too, a clear improvement is achieved over the reference pressure. We hypothesise that this peak shift is a consequence of (i) the model specifying the elastic behaviour of the blood vessels and/or the boundary conditions, (ii) uncertainty of the geometry measurements which are not specific to a given mouse, (iii) a combination of (i) and (ii). The overall model prediction appears better for the hypoxic than the healthy mouse. When the tapering parameter is included in the analysis, a reduction of 31% is registered in the RSS for the control mouse. These results are summarised in Figure 2. Panel (b) illustrates the optimised pressure waveform for the 5D problem plotted alongside that for the 4D case and the measured pressure is superimposed. While the deviation from the measured data has decreased, the offset in the peak value is still present. In order to select between the two

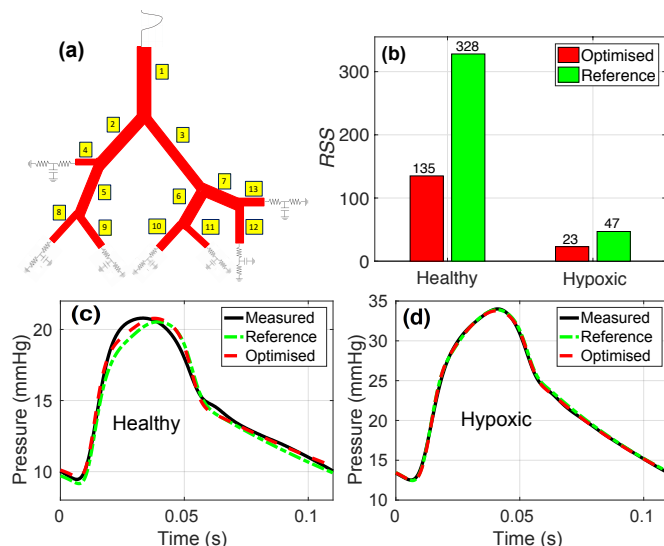


FIGURE 1. (a) The arterial network for the fluid dynamical model, (b) Comparison of RSS between reference and optimised pressure simulations, (c) & (d) Comparison of simulated pressure using reference and optimised parameters values for the healthy and hypoxic mice.

competing models, the 5D model, which includes a tapering parameter, and the 4D one, model selection using the Akaike Information Criterion - AIC (Akaike, 1971) and Bayesian Information Criterion - BIC (Schwarz, 1978) can be performed. However, the estimate of the error variance, σ^2 needed to calculate the log likelihood of the data (5) is not available¹. Hence, we take the inverse approach and calculate what error variance would make us favour the 5D model over the 4D model. Calculations indicate that if $\sigma^2 < 21$, i.e. signal-to-noise ratio, $SNR > 2.40$, then the 5D model is preferred according to the AIC; if $\sigma^2 < 6.06$, i.e. $SNR > 8.30$, then the 5D model is favoured according to the BIC.

In conclusion, parameters have successfully been inferred for this fluid-structure model. Future work will include improvements in the model to capture a more realistic elastic behaviour of the vessel wall. This may address the alignment issue observed near the peak pressure for the healthy mouse by better controlling the steepness of the pressure. Additionally, to account for the uncertainty associated with the geometry measurements, we will estimate them as part of the inference procedure. Finally, we also aim to apply the statistical methods presented here to a population of mice, as well as to data from human patients.

¹In principle, we could infer the variance, but due to the slight model mismatch apparent from Figures 1 and 2, the results would be misleading.

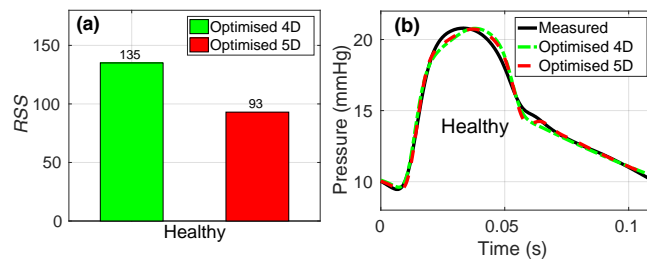


FIGURE 2. (a) Comparison of RSS between the optimised pressure simulations for the healthy mouse, (b) Comparison of simulated pressure using 4D and 5D optimised parameters values for the healthy mouse.

Acknowledgments: This work is part of the research programme of the Centre for multiscale soft tissue mechanics with application to heart & cancer (SoftMech), funded by the Engineering and Physical Sciences Research Council (EPSRC) of the UK, grant reference number EP/N014642/1. Olufsen, Haider and Qureshi were supported by National Science Foundation (NSF-DMS # 1615820). Data were made available by N. Chesler, Department of Biomedical Engineering, University of Wisconsin, Madison.

References

- Akaike, H. (1971), Information theory and an extension of the maximum likelihood principle. In: *Proc. 2nd International Symposium on Information Theory, Tsahkadsor, Armenia, USSR*. 267–281.
- Boggs, P.T. and Tolle, J.W. (2000), Sequential quadratic programming for large-scale nonlinear optimization. *Journal of Computational and Applied Mathematics*, **124(12)**, 123–137.
- Bratley, B. (1988), Algorithm 659: Implementing Sobol’s Quasirandom Sequence Generator. *ACM Trans Math Softw*, **14(1)**, 88–100.
- Qureshi, M.U. et al. (2017), Simulating effects of hypoxia on pulmonary haemodynamics in mice. In: *Proc CMBE*. 271–274.
- Schwarz, G. (1978), Estimating the Dimension of a Model. *Ann. Statist.*, **2(6)**, 461–464.
- Tabima, D.M. et al. (2012), Persistent vascular collagen accumulation alters hemodynamic recovery from chronic hypoxia. *J. Biomech*, **45(5)**, 799–804.
- Yang, K.W. and Lee, T.Y. (2010), Heuristic scaling method for efficient parameter estimation. *Chemical Engineering Research and Design*, **88(56)**, 520–528.